ELSEVIER

Journal of Power Sources 103 (2002) 201–206

JOURNAL OF POWER SOURCES

www.elsevier.com/locate/jpowsour

Elaboration of a new anode material for all-solid state Zn/MnO_2 protonic cells

Laid Telli[a], Abderrezak Hammouche[b,*], Brahim Brahimi[a], Rik W. De Doncker[b]

[a]*Laboratory of Inorganic Materials, M'sila University, 28000 M'sila, Algeria*

[b]*Institute for Power Electronics and Electrical Drives, Aachen University of Technology, Jägerstraße 17-19, D-52066 Aachen, Germany*

Received 23 March 2001; received in revised form 21 June 2001; accepted 21 June 2001

Abstract

A new composite consisting of a mixture of zinc and hydrated ammonium zinc sulfate, Tutton salt, has been elaborated and studied as anode material for all-solid state protonic cells. The results obtained point out the ability of $(NH_4)_2Zn(SO_4)_2{\cdot}6H_2O$ double salt to concomitantly exchange protons with the solid proton conducting electrolyte and accommodate Zn^{2+} cations issued from oxidation. Such features have been evinced by thermal and crystallographic characterizations. The anode composition has been optimized through a kinetic study on a three-electrode type-cell, showing that a 35 wt.% salt-based composite displays the minimum polarization. Zn/MnO_2 cells prepared using such a composite anode achieve relatively high specific capacity and energy of, more than 30 Ah kg^{-1} and 40 Wh kg^{-1}, respectively.

Keywords: All-solid state cell; Composite anode; Zinc; H-montmorillonite; Protonic conductor

1. Introduction

Increasing efforts have recently been devoted to the development of solid state cells using a proton conducting electrolyte. Such systems present outstanding advantages: (a) wider electrolyte stability potential range in comparison with their homologous liquid electrolytes; (b) less electrode corrosion thanks to negligible anionic transference number in the electrolyte and (c) absence of corrosive liquid leakage.

In the last years, many mineral compounds exhibiting fast proton conduction, such as hydrogen uranyl phosphate, phosphotungstic acid and protonated montmorillonite, have been developed for both room temperature power supply applications [1–3] and pH sensing devices [4,5].

The main positive electrode materials employed in solid state protonic batteries are MnO_2 and PbO_2, which are compatible with the tested proton conducting electrolytes and able to accommodate protons [6–8]. MnO_2-based cathode was found to combine high discharge capacity and energy density [9]. However, PbO_2-based cathode composite suffered from poor electrical conductivity [10].

In the early studies on this type of cells, simple metallic elements (Zn, Pb or Fe) have been employed as anode compounds [11,12], but feasibility of ionic exchange at the electrode/electrolyte interface is questionable inasmuch as the anode material must be able to maintain a supply of protons (H^+) during discharge. Hydride materials, such as $TiNiH_x$, present good reversibility, but do not provide sufficient battery emf [13–15]. A zinc-based composite negative electrode, consisting of a mixture of Zn, $ZnSO_4{\cdot}7H_2O$ and $Na_3PO_4{\cdot}12H_2O$, has been proposed by Guitton et al. [16]. It has revealed promising features: the presence of zinc sulfate stabilizes the electrode potential at a value as low as that of the Zn/Zn^{2+} system, and the sodium phosphate is, thanks to its crystallographic equivalent sites and water molecules, responsible for accommodating the produced Zn^{2+} cations on oxidation and for a reversible exchange of protons with the electrolyte. According to Pandey et al. [10], the performances of such a cell could be improved if a metal hydride is used, instead of sodium phosphate, in the composite anode.

In this context, the present work aims at elaborating and characterizing a composite negative electrode consisting of zinc mixed with hydrated ammonium zinc sulfate ($(NH_4)_2Zn(SO_4)_2{\cdot}6H_2O$) Tutton salt. This latter is hereafter denoted by the acronym AZS. Such a double salt would possess, at the same time, both the properties of hosting Zn^{2+} cations issued from oxidation and generating protons by decomposition of its hydration water molecules.

* Corresponding author. Tel.: +49-241-80-69-45; fax: +49-241-67-505.
E-mail address: hm@isea.rwth-aachen.de (A. Hammouche).

0378-7753/02/$ – see front matter
PII: S0378-7753(01)00855-2

2. Experimental

2.1. Syntheses

The hydrated $(NH_4)_2Zn(SO_4)_2{\cdot}6H_2O$ double salt was prepared by evaporating in ambient air at 20°C, a mixture of two equimolar (0.2 mol l^{-1}) aqueous solutions of hydrated zinc sulfate ($ZnSO_4{\cdot}7H_2O$, Prolabo) and anhydrous ammonium sulfate ($(NH_4)_2SO_4$, Prolabo). A week later, large colorless single crystals of many cubic millimeter size were isolated and dried in air. Their shape is depicted by the micrographs of Fig. 1. To be used in the composite anode and for physicochemical analyses, such crystals were ground to produce a 10-μm average grain size powder.

The solid electrolyte used in this investigation is a protonated montmorillonite which was obtained from Na-montmorillonite, following a common procedure consisting in a cationic exchange in a 4 M hydrochloric acid solution, under stirring at 70°C for 2 h [17]. The product was thoroughly washed with distilled water and then dried in air. Its crystalline structure was confirmed by X-ray characterization. The protonic conductivity of H-montmorillonite increased from 10^{-7} to 2.2×10^{-3} S cm^{-1} as relative humidity (RH) rose from 0.2 to 0.9 at 25°C [3,18].

H-montmorillonite samples were settled, before use, for 7 days inside a glass container where RH could be varied within a wide range of 0.1–0.9 in contact with appropriate water–sulfuric acid mixtures [19], and monitored by means of an HR270-type thermohygrometer.

2.2. Techniques of physicochemical characterization

X-ray examination was carried out on AZS powder by means of a Philips PM8209 diffractometer using Cu Kα radiation.

TGA and DTA were performed with a Labsys TG DTA 16 Setaram instrument. Experiments were run in nitrogen atmosphere, with a heating rate of 5°C min^{-1}, in the 20–1000°C temperature range.

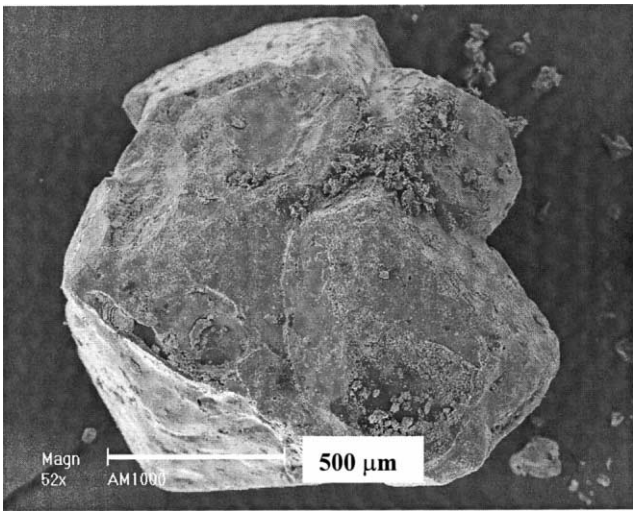

Fig. 1. Scanning electron micrograph of a $(NH_4)_2Zn(SO_4)_2{\cdot}6H_2O$ crystal.

2.3. Cell preparation and electrochemical characterization

The electrochemical cells were assembled by successively pressing the anode, electrolyte and the cathode compositions in the same palletizing die to obtain a pellet of 13 mm diameter and 2 mm thickness. At first, the desired negative active mass (200 mg), consisting of a blend of Zn (Riedel-de Haen) and AZS in a given mass ratio, was obtained by gentle pressure. A weighed amount (200 mg) of electrolyte powder was poured over the precompacted anode and the assembly was again pressed mildly. Subsequently, a known amount (200 mg) of the positive active mass, consisting of manganese dioxide (chemical γ variety, Sedema), was added and the entire assembly compacted at 7 ton cm^{-2}. Finally, the cell was assembled in a holder and placed in a container with a fixed internal RH.

Electrochemical three-electrode cells were prepared to allow the separate evaluation of both anode and cathode polarizations in these all-solid state cells during operation. A comparison electrode was produced by splitting the anode layer into two equal parts, following the procedure described elsewhere [20]. During discharge, one of these parts, which is crossed by the current, acts as a working electrode (surface area = 0.45 cm^2) while the other, staying at its equilibrium state, plays the role of a comparison electrode. Cell voltage and half-cell potentials were continuously recorded for the duration of the test.

After fabrication, the cells were allowed to stabilize for 18 h after which their voltage became constant. The average cell voltage amounted to 1.81 V. Electrochemical measurements were carried out using a Radiometer PGP 201-type galvanostat and recorded through a BBC Gorez Metrawatt SE 120 recorder.

3. Results and discussion

3.1. X-ray examination

The X-ray diffraction pattern recorded for $(NH_4)_2Zn(SO_4)_2{\cdot}6H_2O$ (Fig. 2) is very similar to that of single-phase AZS salt given in the JCPDS files (ASTM 35-0767). It crystallizes in the monoclinic system with unit cell parameters ($a = 6.251$ Å, $b = 12.517$ Å, $c = 9.239$ Å and $\beta = 106.834°$) very close to those reported by Cotton et al. [21,22] for the same compound.

3.2. Thermal analyses

TGA and DTA curves obtained for the $(NH_4)_2Zn(SO_4)_2{\cdot}6H_2O$ salt are shown in Fig. 3. In the first step of thermal decomposition, which starts at 60°C and extends to 125°C,

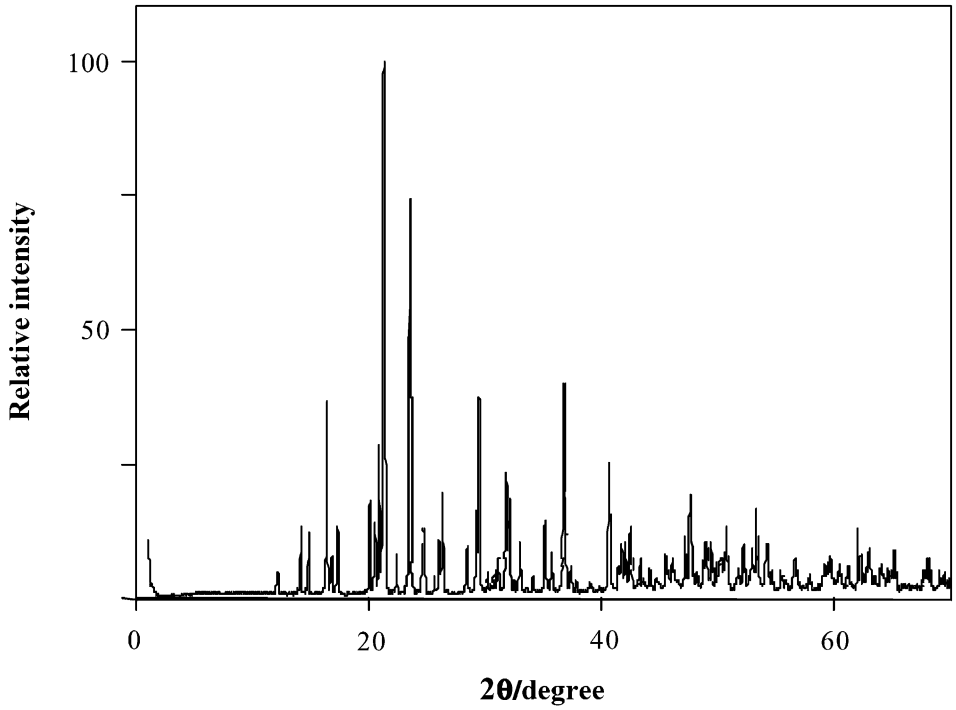

Fig. 2. X-ray diffraction pattern of $(NH_4)_2Zn(SO_4)_2{\cdot}6H_2O$ powder.

the tested sample loses its hydration water. The weight loss is estimated at 27.3%, corresponding precisely to six water molecules per salt unit. Simultaneously, the DTA curve shows a strong endothermic peak around 120°C. Since this hydration state is thermally stable below 60°C, the compound is expected to exhibit stable and reproducible behavior in cells operating near ambient temperature. In the 260–440°C temperature range, a further 31.7% weight loss occurs in closely consecutive stages, corresponding to decomposition of $(NH_4)_2Zn(SO_4)_2$ into zinc sulfate, producing NH_3, H_2O and SO_3 [23]. The DTA curve shows three endothermic peaks in this temperature range. Finally, between 650 and 1000°C, a further weight loss of 20.8% is observed corresponding to the decomposition of zinc sulfate, producing ZnO, SO_2 and O_2. This process is accompanied by two endothermic DTA peaks. The recorded total weight loss for the three steps of decomposition is 79.8%, giving the solid state zinc oxide as a final product. These data also confirm the chemical composition of the Tutton salt herein synthesized.

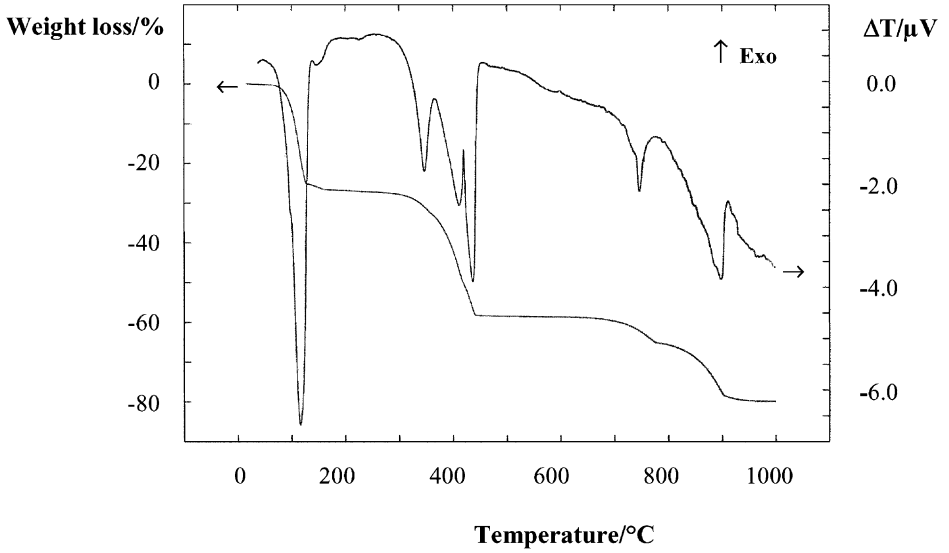

Fig. 3. TGA and DTA curves of $(NH_4)_2Zn(SO_4)_2{\cdot}6H_2O$. Atmosphere: N_2, heating rate: 5°C min^{-1}.

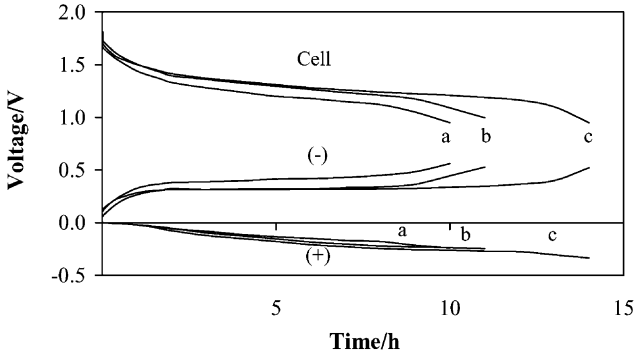

Fig. 4. Evolution of cell voltage (Cell), anodic polarization (−) and cathodic polarization (+) at 1.00 mA cm^{-2} and RH = 0.9 of Zn/H-montmorillonite/MnO_2 three-electrode type cells prepared with different negative active mass compositions (Zn:AZS in wt.%): (a) 85:15; (b) 50:50; (c) 65:35.

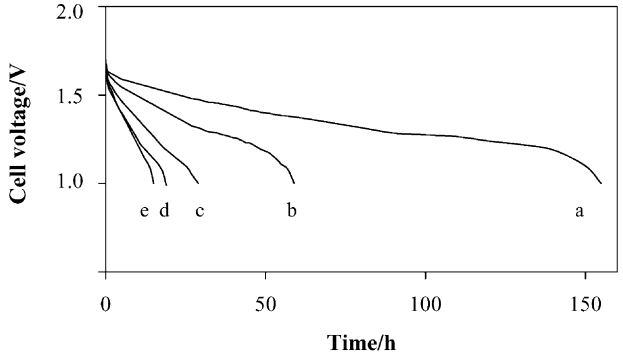

Fig. 6. Discharge characteristics of complete cells performed at RH = 0.9 for different current densities (mA cm^{-2}): (a) 0.1; (b) 0.25; (c) 0.5; (d) 0.75; (e) 1.0.

3.3. Discharge characteristics

3.3.1. Optimization of the negative active mass composition

The discharge characteristics, at an anodic current density of 1.00 mA cm^{-2}, of some typical three-electrode type cells with identical positive electrodes, but negative electrodes of different compositions are given in Fig. 4. Note that unbalance in anode and cathode polarizations partly resulted from the unequal electrodes surface areas. The composition of the negative active mass, which consisted of a blend of Zn and AZS, was optimized by varying the mass ratio in the 10–90% AZS range, everything else being equal. These AZS-based systems display proper behavior with experimental specific capacities reaching 30 Ah kg^{-1}, when referred to the total mass of the cell. The experimentally retrieved capacity reached maximum values for anodes containing about 35% AZS, as shown in Fig. 5. Mixtures using too little of either AZS or Zn gave results, about three-fold inferior, similar to those reported for anodes containing only the metal element [9,10]. Such a behavior evinces the requisite role of the ammonium zinc sulfate double salt in the electrode kinetics. The maximum capacity was actually observed for that mixture exhibiting nearly equal grains surface areas of both constituents; these can merely be estimated from their respective densities ($d_{Zn} = 7.14$ and $d_{AZS} = 1.93$) [24] and average grain sizes ($\phi_{Zn} = 5$ μm and $\phi_{AZS} = 10$ μm). Thus, a maximum contact area and accordingly, a minimum voltage loss were expected for such a composite.

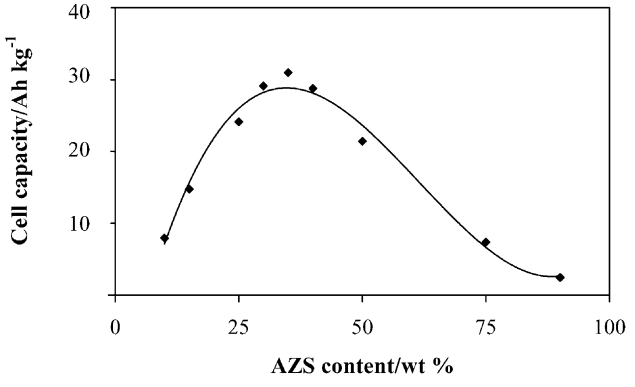

Fig. 5. Variation of discharge capacity with composition of the composite anode mass at 1.00 mA cm^{-2} and RH = 0.9.

Discharges were performed on two-electrode type cells using the optimum anode composition, with current densities varying from 0.1 to 1.0 mA cm^{-2} down to 1.0 V (Fig. 6). The experimentally obtained characteristics, summarized in Table 1, appear much more interesting than those reported in the literature for similar all-solid state type systems [9,10,16,25], exhibiting particularly a little variation over a current density decade. Further improvement of such performances may even be achieved by optimizing the masses of the cell constituents.

Under relative humidities of 0.75 and medium current densities (up to 0.5 mA cm^{-2}), still high capacities (20 Ah kg^{-1}) were obtained. But for lower humidities, a rapid decrease in the capacity occurred. Such a deterioration is ascribable to dehydration of the electrolyte which suffered from poor electrical conductivity [3,18]. The composite anode remained stable, since the sulfate double salt shows a fixed hydration stoichiometry over the 0.1–0.9 RH range.

3.3.2. Mechanism of the anodic reaction

The anode potential curves disclosed in Fig. 4 are typically wave shaped, suggesting that the negative active mass acts as a solid solution in this potential range. According to

Table 1
Discharge performances of complete cells at different current densities, RH = 0.9 and for a cut-off voltage of 1.0 V

i (mA cm^{-2})	C (Ah kg^{-1})	W (Wh kg^{-1})
0.1	33.2	43.3
0.25	32.6	41.0
0.5	32.1	40.9
0.75	31.5	42.1
1.0	30.9	42.1

the mechanism of anodic reaction proposed for this type of electrodes [16], the sulfate double salt would be able to exchange H^+ with the solid proton conducting electrolyte and accommodate Zn^{2+} cations issued from oxidation of zinc. The overall reaction can be regarded as an insertion process for Zn^{2+} cations.

$$x\mathrm{Zn} + \langle (\mathrm{NH_4})_2\mathrm{Zn}(\mathrm{SO_4})_2 \cdot 6\mathrm{H_2O}\rangle \rightarrow \langle (\mathrm{NH_4})_2\mathrm{Zn}_{1+x}(\mathrm{SO_4})_2(6-2x)\mathrm{H_2O} \cdot 2x(\mathrm{OH})\rangle + 2x\,\mathrm{H}^+ + 2x\,\mathrm{e}^-$$

This statement is evinced by X-ray examination of the composite anode at different states of discharge, which showed no extra peaks due to formation of any new crystalline phase, for instance, zinc hydroxide, except those of the Zn and AZS mixture. Formation of solid solution upon insertion seems to be likely since there appears to be room in the AZS crystalline structure [26].

In order to point out the role of the structure of the double salt phase in inserting Zn^{2+} cations, cells were fabricated by successively substituting for AZS in the composite anode an equivalent quantity of each of the starting materials (i.e. $ZnSO_4{\cdot}7H_2O$ and $(NH_4)_2SO_4{\cdot}nH_2O$) and their mixture, all being hydrated and presenting close morphology characteristics to those of AZS. The relevant discharge curves shown in Fig. 7, gave capacities not exceeding 20% of that obtained with AZS. This point gives supporting evidence of the role of the double salt structure in accommodating Zn^{2+} cations; the other tested salts manifest less ability for such an insertion process.

During the anodic process, protons must also be supplied by the negative electrode bulk. In this respect, both ammonium cations and hydration water molecules may be expected to provide them. Identifying the actual source of protons was achieved by substituting for AZS in the composite anode an equivalent quantity of potassium zinc sulfate $K_2Zn(SO_4)_2{\cdot}6H_2O$. Hydrated potassium zinc sulfate is also a Tutton salt which was prepared in the same experimental conditions as for AZS. The discharge characteristic plotted

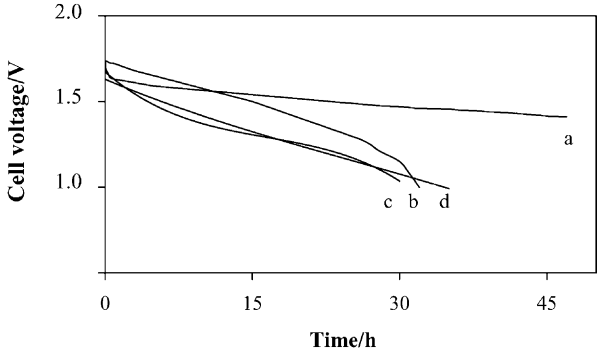

Fig. 7. Discharge characteristics of complete cells at 0.1 mA cm^{-2} and RH = 0.9, fabricated by substituting for AZS (a) in the composite anode, an equivalent quantity of (b) $ZnSO_4{\cdot}7H_2O$, (c) $(NH_4)_2SO_4{\cdot}nH_2O$, (d) mixture of $ZnSO_4{\cdot}7H_2O$ and $(NH_4)_2SO_4{\cdot}nH_2O$.

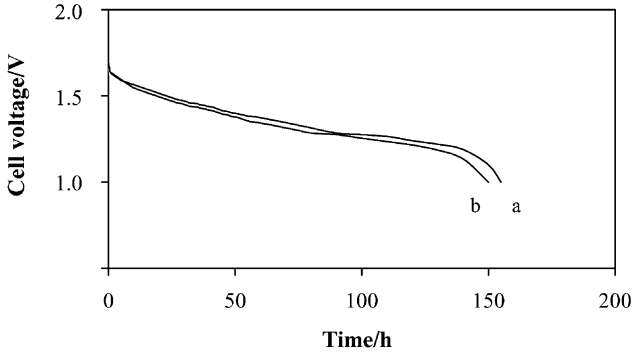

Fig. 8. Discharge characteristics of complete cells at 0.1 mA cm^{-2} and RH = 0.9, fabricated by replacing AZS (a) in the composite anode with $K_2Zn(SO_4)_2{\cdot}6H_2O$ (b).

in this case (Fig. 8) is nearly identical to that obtained using AZS, indicating that protons are generated during oxidation exclusively by hydration water molecules according to the aforementioned overall reaction; the ammonium cations do not seemingly take part in it. This result states that for proper functioning, such an anode constituent must be hydrated and in this respect, the stable hydration state of ammonium zinc sulfate over a wide range of RH is viewed as a virtue. The largest capacity observed in the present tests (ca. 30 Ah kg^{-1}) involves four water molecules among the six structural water molecules per salt unit.

4. Conclusion

It has been established that hydrated ammonium zinc sulfate, associated to zinc, produces a composite anode for all-solid state Zn/MnO_2 cells that achieve relatively high specific capacity and energy. Such a double salt presents the likely ability to simultaneously exchange H^+ with the solid proton conducting electrolyte and accommodate Zn^{2+} cations resulting from oxidation, at a durable potential. This statement was based on thermal analysis data and evinced by X-ray examination of the composite anode at different states of discharge. It can be inferred from the present results that such features are fairly common to some of the hydrated Tutton salts. The obtained data, although still to be optimized, is promising. These systems deserve further investigation by both optimizing the mass of the cell constituents, on the one hand, and assembling a hydrated double salt-based composite anode with other appropriate electrolyte and positive electrode materials, on the other hand.

Acknowledgements

Thanks are due to Dr. A. Merrouche, Researcher of the Laboratory of Inorganic Materials (M'sila University) and to Researchers of the Laboratory of Mineral Materials (Mulhouse University, France) for their assistance in materials characterizations.

References

[1] A.T. Howe, M.G. Shilton, J. Solid State Chem. 28 (1979) 345.
[2] N. Giordano, P. Staiti, S. Hocevar, A.S. Arico, Electrochim. Acta 41 (1996) 397.
[3] N. Aliouane, A. Hammouche, M. Boutahala, Extended abstract, in: Proceedings of the 9th International Conference on Solid State Protonic Conductors, Bled, Slovenia, 17–21 August 1998.
[4] L. Zerroual, L. Telli, Sens. Actuators B 24/25 (1995) 741.
[5] L. Telli, B. Brahimi, A. Hammouche, Solid State Ionics 128 (2000) 255.
[6] H. Kahil, E.J.L. Schouler, M. Forestier, J. Guitton, Solid State Ionics 18/19 (1986) 892.
[7] C. Poinsignon, Y. Chabre, J. Pannetier, M. Ripert, A. Denoyelle, J.Y. Sanchez, Journées Européennes d'Etudes de la S.E.E, in: Accumulateurs Electrochimiques, Evolution et Techniques Récentes, Gif-sur-Yvette, France, 21–22 November 1989.
[8] N. Chelali, J. Guitton, Solid State Ionics 73 (1994) 227.
[9] K. Singh, R.U. Tiwari, Solid state ionic materials, in: Proceedings of the 4th Asian Conference on Solid State Ionics, Kuala Lumpur, Malaysia, 2–6 August 1994.
[10] K. Pandey, N. Lakshmi, S. Chandra, J. Power Sources 76 (1998) 116.
[11] G.W. Mellors, Eur. Patent No. 013120 A2.
[12] T. Takahashi, S. Tanase, O. Yamamoto, J. Appl. Electrochem. 10 (1980) 415.
[13] E.W. Justi, H. Ewe, A.W. Kalberlah, Energy Conv. 10 (1970) 183.
[14] P. de Lamberterie, A. Rouault, R. Fruchart, M. Forestier, J. Guitton, in: Proceedings of the 5th International Symposium on the Properties and Applications of Metal Hydrides, Maubuisson, France, 25–30 May 1986.
[15] P. de Lamberterie, M. Forestier, J. Guitton, A. Rouault, R. Fruchart, D. Fruchart, C. R. Acad. Sci. Paris, Sec. II 300 (1985) 663.
[16] J. Guitton, B. Dongui, R. Mosdale, M. Forestier, Solid State Ionics 28–30 (1988) 847.
[17] S.H. Sheffield, A.T. Howe, Mater. Res. Bull. 14 (1979) 929.
[18] N. Aliouane, A. Hammouche, L. Telli, M. Boutahala, B. Brahimi, Solid State Ionics, submitted for publication.
[19] P. Pascal, Nouveau Traité de Chimie Minérale, Vol. 13-2, Masson, Paris, 1961, p. 1338.
[20] A. Hammouche, J.P. Caire, N. Chelali, M. Boutahala, Electrochim. Acta 42 (1997) 2511.
[21] F.A. Cotton, L.M. Daniels, C.A. Murillo, J.F. Quesada, Inorg. Chem. 32 (1993) 4861.
[22] F.A. Cotton, L.M. Daniels, L.R. Falvello, C.A. Murillo, A.J. Schultz, Inorg. Chem. 33 (1994) 5396.
[23] J. Slivnik, A. Rahten, D. Gantar, Croat. Chem. Acta 58 (1985) 289.
[24] R.C. Weast (Ed.), Handbook of Chemistry and Physics, 69th Edition, CRC Press, Boca Raton, FL, 1988–1989.
[25] K. Singh, R.U. Tiwari, V.K. Deshpande, J. Power Sources 46 (1993) 65.
[26] M.A. Araya, F.A. Cotton, L.M. Daniels, L.R. Falvello, C.A. Murillo, Inorg. Chem. 32 (1993) 4853.